

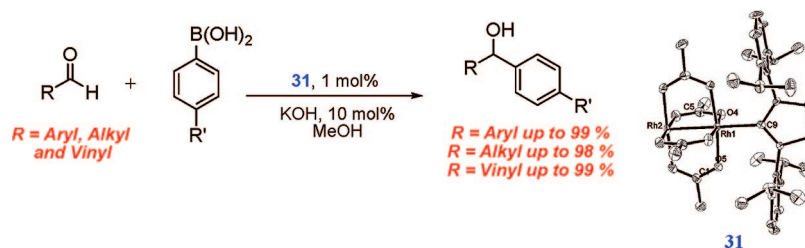
Axial Coordination of NHC Ligands on Dirhodium(II) Complexes: Generation of a New Family of Catalysts

Alexandre F. Trindade,[†] Pedro M. P. Gois,^{*,†,‡,§} Luís F. Veiros,[†] Vânia André,[†] M. Teresa Duarte,[†] Carlos A. M. Afonso,[†] Stephen Caddick,[‡] and F. Geoffrey N. Cloke[§]

CQFM and CQE, Departamento de Engenharia Química e Biológica, Complexo I, Instituto Superior Técnico, Av. Rovisco Pais 1, 1049-001 Lisboa, Portugal, Department of Chemistry, University College London, 20 Gordon Street, London WC1H 0AJ, U.K., and Department of Chemistry, School of Life Sciences, University of Sussex, Falmer, Brighton BN1 9QJ, U.K.

pedrogois@ist.utl.pt

Received January 14, 2008



An efficient new methodology for the arylation of aldehydes is disclosed which uses dirhodium(II) catalysts and *N*-heterocyclic carbene (NHC) ligands. Complexes of Rh₂(OAc)₄ with one and two NHCs attached on the axial positions were successfully isolated, fully characterized, and used as catalysts in the reaction. The saturated monocomplex ((NHC **5**)Rh₂(OAc)₄) **31** was shown to be the most active catalyst and was particularly efficient in the arylation of alkyl aldehydes. DFT calculations support participation of complexes with one axial NHC in the reaction as the catalysts active species and indicate that hydrogen bonds involving dirhodium unit, reactants, and solvent (alcohol) play an important role on the reaction mechanism.

Introduction

Dirhodium(II) complexes have,¹ during the years, gathered considerable interest from the organic chemistry community as they exhibit remarkable catalytic activity in transformations such as intramolecular and intermolecular C–H bond activation with Rh(II) carbenoids,² C–H bond amination with Rh(II) nitrenoids, oxidations, cycloadditions, and a variety of ylide-based transformations.³

The recognized success of this class of complexes relies on their Rh(II) bimetallic structure. They have a Rh–Rh bond and four bridging ligands, responsible for controlling the catalyst

electrophilicity and in some cases provide a mechanism for inducing asymmetry.^{1,2} The two axial ligands (normally solvent molecules, Scheme 1) are generally considered to have a less important role in catalysis as they form a much weaker bond with the electrophilic center and, for that reason, are easily displaced from the rhodium active centers.^{1,2}

Despite the fact that the contribution of the axial ligands to the overall reactivity of dirhodium complexes has generally been overlooked, some important insights were recently presented.

(3) Selected examples: (a) Catino, A. J.; Forslund, R. E.; Doyle, M. P. *J. Am. Chem. Soc.* **2005**, *126*, 13622–13623. (b) Catino, A. J.; Nichols, J. M.; Choi, H.; Gottipamula, S.; Doyle, M. P. *Org. Lett.* **2005**, *7*, 5167–5170. (c) Liang, C.; Peillard, F. R.; Fruit, C.; Müller, P.; Dodd, R. H.; Dauban, P. *Angew. Chem., Int. Ed.* **2006**, *45*, 4641–4644. (d) Reddy, R. R.; Davies, H. M. L. *Org. Lett.* **2006**, *8*, 5013–5016. (e) Fiori, K. W.; Du Bois, J. J. *Am. Chem. Soc.* **2007**, *129*, 562–568. (f) Anada, M.; Tanaka, M.; Washio, T.; Yamawaki, M.; Abe, T.; Hashimoto, S. *Org. Lett.* **2007**, *9*, 4559–4562. (g) Doyle, M. P.; Valenzuela, M.; Huang, P. *Proc. Nat. Acad. Sci. U.S.A.* **2004**, *101*, 5391–5395. (h) Anada, M.; Washio, T.; Shimada, N.; Kitagaki, S.; Nakajima, M.; Shiro, M.; Hashimoto, S. *Angew. Chem., Int. Ed.* **2004**, *43*, 2665–2668. (i) Forslund, R. E.; Cain, J.; Colyer, J.; Doyle, M. P. *Adv. Synth. Catal.* **2005**, *347*, 87–92. (j) Washio, T.; Nakamura, S.; Anada, M.; Hashimoto, S. *Heterocycles* **2005**, *66*, 567–578. (k) Wang, Y.; Wolf, J.; Zavalij, P.; Doyle, M. P. *Angew. Chem., Int. Ed.* **2008**, *47*, 1439–1442. (l) Catino, A. J.; Nichols, J. M.; Gorslund, R. E.; Doyle, M. P. *Org. Lett.* **2005**, *7*, 2787–2790.

[†] Instituto Superior Técnico.

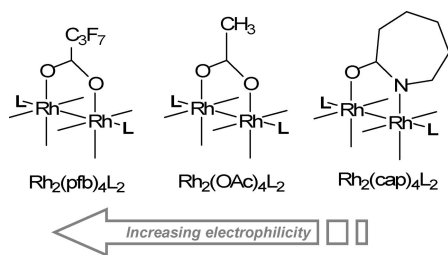
[‡] University College London.

[§] University of Sussex.

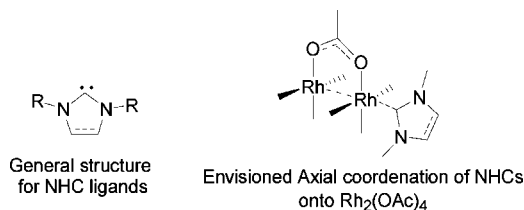
(1) (a) Doyle, M. P.; McKervey, M. A.; Ye, T. *Modern Catalytic Methods for Organic Synthesis with Diazo Compounds*; Wiley-Interscience: New York, 1998. (b) Lou, Y.; Remarchuk, T. P.; Corey, E. J. *J. Am. Chem. Soc.* **2005**, *127*, 14223–14230. (c) Cotton, F. A.; Hillard, E.; Murillo, C. A. *J. Am. Chem. Soc.* **2002**, *124*, 5658–5660.

(2) (a) Davies, H. M. L.; Beckwith, R. E. *J. Chem. Rev.* **2003**, *103*, 2861–2903. (b) Doyle, M. P. *J. Org. Chem.* **2006**, *71*, 9253–9260. (c) Gois, P. M. P.; Afonso, C. A. M. *Eur. J. Org. Chem.* **2004**, 3773, 3788.

SCHEME 1



SCHEME 2



Doyle et al. disclosed a paramagnetic dirhodium(II, III) caprolactam complex generated from one-electron oxidation of $\text{Rh}_2(\text{cap})_4$ in the presence of *N*-bromosuccinimide (NBS). This new mixed-valent complex with a bromide attached in the axial position proved to be an excellent catalyst to perform the aziridination of olefins.³¹

Therefore, we hypothesized that the reactivity of these dirhodium(II) complexes could be effectively tuned by incrementing the electronic density of the terminal Rh atom by simple coordination with the appropriate axial ligand. If successful, this approach would considerably enhance the already remarkable activity of this family of complexes. Among all possibilities, *N*-heterocyclic carbenes (NHCs) seemed to offer good potential as appropriate ligands for this propose as they are neutral, two-electron donor (σ -donating) ligands with negligible π -back bonding tendency (Scheme 2).⁴

This report follows our preliminary study on the arylation of aldehydes with aryl boronic acids catalyzed by dirhodium(II) complexes and NHCs.⁵

Results and Discussion

The arylation of aldehydes has recently received considerable attention because diaryl methanols are key structural elements in an array of pharmacologically active compounds and are, for that reason, important synthetic targets.⁶ In 2001, Fürstner et al. described the Rh–NHC-catalyzed addition of boronic acids to aldehydes and reported that RhCl_3 is an excellent source of rhodium for this transformation.⁷ Inspired by this pivotal work, we were delighted to observed that upon combining $\text{Rh}_2(\text{OAc})_4$

with NHC (**4**, **5**, **6**) precursors, the secondary alcohol **3** was obtained almost quantitatively in less than 1 h using phenylboronic acid as the phenyl-transfer reagent. Unexpectedly, all the imidazolium salts containing *N*-aryl substituents afforded the desired product despite having different steric (**4** and **6**) and electronic profiles (**8**–**11**),⁸ whereas salts with bulky *N*-alkylic substituents (**8**–**11**) did not react at all even after prolonged heating (Table 1, entries 7–10). This fact suggested a possible conflict between the bulky *N*-alkylic substituents and the dirhodium(II) bridging ligands.⁵ This idea was given further support by the finding that the considerably less bulky 1,3-dimethylimidazolium iodide salt **7** afforded the alcohol **3** in 43%. NHCs are often regarded as phosphines surrogates, though in this particular system, they performed much better than phosphines **12**–**14** (Table 1, entries 11–13).

One of the most important characteristics of dirhodium(II) complexes is the fact that they are easily tunable in their electrophilicity profile (Scheme 1) which dramatically reflects on the catalyst reactivity and selectivity.^{1,2} Therefore, different Rh(II) catalysts with diverse electronic characters were tested. At 90 °C, all catalysts afforded the alcohol in excellent yields, though, when the temperature was decreased to 60 °C, only the complex dirhodium(II) perfluorobutyrate ($\text{Rh}_2(\text{pfb})_4$), with electron-withdrawing bridging ligands, successfully afforded alcohol **3** (Table 2, entries 3 and 6).

Once the most efficient dirhodium complex had been identified, the reaction conditions were evaluated, with a particular emphasis on solvent effects. The protic solvent *tert*-amyl alcohol proved to be an excellent medium for this in situ protocol allowing the formation of secondary alcohol **3** at temperatures as low as 40 °C (Table 3, entries 2–4). This effect was also observed when using other alcohols such as MeOH (Table 3, entry 9).

The optimized protocol was tested in the arylation of aldehydes with different steric and electronic properties as shown in Table 4. The reaction proceeded, in most cases, with notable efficiency (up to 99% isolated yield) under considerably milder conditions than other systems based on rhodium complexes and NHC ligands.⁹ The in situ methodology demonstrated a noteworthy tolerance to functional groups, although it is highly sensitive to steric and electronic effects. In direct contrast to other catalytic systems,¹⁰ electron-donating groups at the *para* position of the aryl aldehyde activated the aldehyde (Table 4, entry 4), while strong electron-withdrawing groups (Table 4, entries 8 and 9) deactivated the aldehyde as well as the boronic acid (Table 4, entry 18). Generally, aldehydes possessing electron-withdrawing groups required higher temperatures to achieve higher conversions; this was the case of *p*-nitrobenzaldehyde which at 60 °C afforded only 49% of the desired alcohol while at 80 °C the arylated product was isolated in 77% yield (Table 4, entries 11 and 12).

(4) (a) Hahn, F. E. *Angew. Chem., Int. Ed.* **2006**, *45*, 1348–1352. (b) Herrmann, W. A. *Angew. Chem., Int. Ed.* **2002**, *41*, 1290–1309. (c) Glorius, F., Ed. *N-Heterocyclic Carbenes in Transition Metal Catalysis*. *Top. Organomet. Chem.* **2007**, *21*. (d) Nolan, S. P., Ed. *N-Heterocyclic Carbenes in Synthesis*; Wiley-VCH: Weinheim, 2006.

(5) (a) Gois, P. M. P.; Trindade, A. F.; Veiros, L. F.; Andre, V.; Duarte, M. T.; Afonso, C. A. M.; Caddick, S.; Cloke, F. G. N. *Angew. Chem., Int. Ed.* **2007**, *46*, 5750–5753. (b) During the preparation of this manuscript, the following paper regarding NHC–Rh(II) complexes was disclosed: Nae, S. J.; Lee, B. Y.; Bui, N.-N.; Mho, S.-i.; Jang, H.-Y. *J. Organomet. Chem.* **2007**, *692*, 5523–5527.

(6) (a) Schmidt, F.; Stemmler, R. T.; Rudolph, J.; Bolm, C. *Chem. Soc. Rev.* **2006**, *35*, 454–470. (b) Fagnou, K.; Lautens, M. *Chem. Rev.* **2003**, *103*, 169–196. (c) Bolm, C.; Hildebrand, J. P.; Muñoz, K.; Hermanns, N. *Angew. Chem., Int. Ed.* **2001**, *40*, 3284–3308.

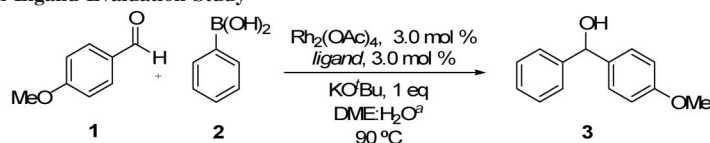
(7) Fürstner, A.; Krause, H. *Adv. Synth. Catal.* **2001**, *343*, 343–350.

(8) Dorta, R.; Stevens, E. D.; Scott, N. M.; Costabile, C.; Cavallo, L.; Hoff, C. D.; Nolan, S. P. *J. Am. Chem. Soc.* **2005**, *127*, 2485–2495.

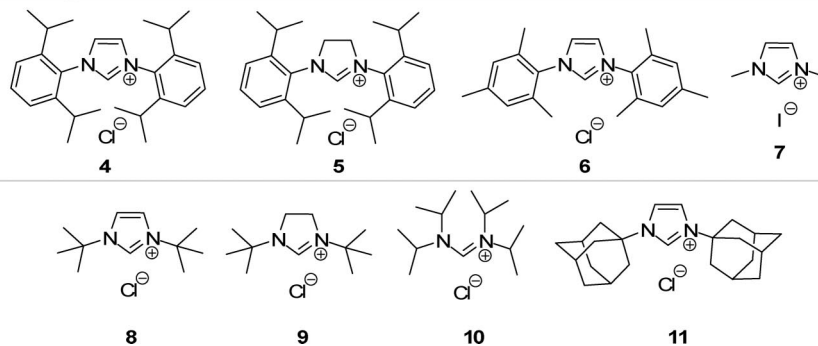
(9) Selected examples: (a) Yan, C.; Zeng, X.; Zhang, W.; Luo, M. *J. Organomet. Chem.* **2006**, *691*, 3391–3396. (b) Imlinger, N.; Mayr, M.; Wang, d.; Wurst, K.; Buchmeiser, M. R. *Adv. Synth. Catal.* **2004**, *346*, 1836–1843. (c) Ozdemir, I.; Demir, S.; Çetinkaya, B.; Çetinkaya, E. *J. Organomet. Chem.* **2005**, *690*, 5849–5855. (d) Focken, T.; Rudolph, J.; Bolm, C. *Synthesis* **2005**, *3*, 425–428. (e) Yan, C.; Zeng, X.; Luo, M. *J. Organomet. Chem.* **2006**, *691*, 3391–3396. (f) Becht, J.-M.; Bappert, E.; Helmchen, G. *Adv. Synth. Catal.* **2005**, *347*, 1495–1498.

(10) (a) Ueda, M.; Miyaura, N. *J. Org. Chem.* **2000**, *65*, 4450–4452. (b) Jagt, R. B. C.; de Vries, J. G.; Feringa, B. L.; Minnard, A. J. *Org. Biomol. Chem.* **2006**, *4*, 773–775.

TABLE 1. In Situ Method: Axial Ligand Evaluation Study



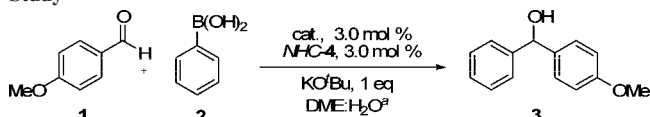
Axial Ligands: NHC Precursors



entry	dirhodium(II) catalyst	ligands	time (h)	yield ^b (%)
1		NHC 4	20	traces
2	Rh ₂ (OAc) ₄		20	n.r.
3	Rh ₂ (OAc) ₄	NHC 4	0.5	94
4	Rh ₂ (OAc) ₄	NHC 5	1	99
5	Rh ₂ (OAc) ₄	NHC 6	1	97
6	Rh ₂ (OAc) ₄	NHC 7	24	43
7	Rh ₂ (OAc) ₄	NHC 8	20	n.r.
8	Rh ₂ (OAc) ₄	NHC 9	20	n.r.
9	Rh ₂ (OAc) ₄	NHC 10	20	n.r.
10	Rh ₂ (OAc) ₄	NHC 11	20	traces
11	Rh ₂ (OAc) ₄	12, P(Ph) ₃	20	37
12	Rh ₂ (OAc) ₄	13, P(^t Bu) ₃	24	20
13	Rh ₂ (OAc) ₄	14, P(ⁿ Bu) ₃	4	52 ^c

^a DME/H₂O (0.5:0.12 mL). ^b Isolated yields after purification by preparative thin-layer chromatography. ^c Complete conversion. n.r. = no reaction. Rh₂(pfb)₄: rhodium(II) heptafluorobutyrate dimer. Rh₂(Ooct)₄: rhodium(II) octanoate dimer. Rh₂(cap)₄: dirhodium(II) caprolactam dimer.

TABLE 2. In Situ Method: Dirhodium(II) Catalyst Evaluation Study



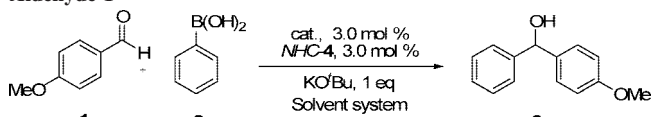
entry	dirhodium(II) catalyst	T (°C)	time (h)	yield ^b (%)
1	Rh ₂ (OAc) ₄	90	0.5	94
2	Rh ₂ (octanoate) ₄	90	6	92
3	Rh ₂ (pfb) ₄	90	0.5	95
4	Rh ₂ (cap) ₄	90	0.5	90
5	Rh ₂ (OAc) ₄	60	24	n.r.
6	Rh ₂ (pfb) ₄	60	24	83
7	Rh ₂ (cap) ₄	60	24	n.r.
8 ^c	Rh ₂ (OAc) ₄	90	1	traces

^a DME/H₂O (0.5:0.12 mL). ^b Isolated yields after purification by preparative thin layer chromatography. n.r. = no reaction. ^c Reaction carried out with 1 mol% of catalyst and ligand.

The optimized procedure is not limited to aryl aldehydes; thus, aliphatic aldehydes also react smoothly with phenylboronic acid, even if they are sterically hindered. This is highlighted with cyclohexanecarboxaldehyde which afforded the alcohol in 88% yield (Table 4, entries 19 and 20).

The reaction of 2-naphthaldehyde at 60 °C afforded the secondary alcohol in 56% yield after 24 h, though the same substrate at 80 °C resulted in almost complete conversion to

TABLE 3. In Situ Method: Solvent Effect on the Arylation of Aldehyde 1

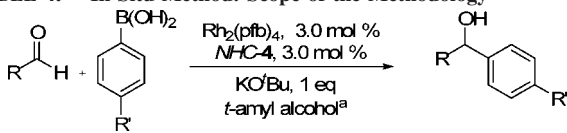


entry	dirhodium(II) catalyst	solvent system	T (°C)	time (h)	yield ^b (%)
1	Rh ₂ (OAc) ₄	DME	90	6	n.r.
2	Rh ₂ (pfb) ₄	<i>tert</i> -amyl alcohol	60	0.5	94
3	Rh ₂ (pfb) ₄	<i>tert</i> -amyl alcohol	40	0.5	90
4	Rh ₂ (pfb) ₄	<i>tert</i> -amyl alcohol	r.t.	24	n.r.
5	Rh ₂ (pfb) ₄	toluene/H ₂ O ^a	60	24	46
6	Rh ₂ (pfb) ₄	DME/H ₂ O ^a	60	24	83
7	Rh ₂ (pfb) ₄	DME/ ⁿ BuOH	60	24	24
8	Rh ₂ (pfb) ₄	CH ₃ CN	60	24	n.r.
9	Rh ₂ (pfb) ₄	MeOH	60	5	92
10	RhCl ₃	<i>tert</i> -amyl alcohol	40	0.5	n.r.

^a Organic solvent/H₂O (0.5:0.12 mL). ^b Isolated yields after purification by preparative thin-layer chromatography. n.r. = no reaction.

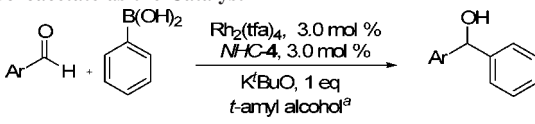
the desired product (Table 4, entries 14 and 15). These results may indicate that bulky aryl aldehydes encounter steric hindrance as they approach the Rh active center. Therefore, we envisioned that by reducing the volume of the complex bridging ligands this effect would be attenuated. In fact, by performing the reaction in the presence of dirhodium(II) trifluoroacetate

TABLE 4. In Situ Method: Scope of the Methodology



entry	R	R'	product	T (°C)	time (h)	yield ^b (%)
1	C ₆ H ₅	H	15	60	1	99
2	<i>p</i> -MeC ₆ H ₄	H	16	60	4	91
3	2,6-Me ₂ C ₆ H ₃	H	17	60	1	70
4	<i>p</i> -MeOC ₆ H ₄	H	3	40	0.5	90
5	<i>p</i> -MeOC ₆ H ₄	H	3	60	0.5	94
6	<i>p</i> -ClC ₆ H ₄	H	18	60	0.7	95
7	<i>p</i> -BrC ₆ H ₄	H	19	60	5	84
8	<i>p</i> -FC ₆ H ₄	H	20	60	5	77
9	<i>p</i> -CNC ₆ H ₄	H	21	60	4	55
10	<i>p</i> -CNC ₆ H ₄	H	21	80	5	80
11	<i>p</i> -NO ₂ C ₆ H ₄	H	22	60	22	49
12	<i>p</i> -NO ₂ C ₆ H ₄	H	22	80	5	77
13	<i>p</i> -PhC ₆ H ₄	H	23	60	1	99
14	2-naphthyl	H	24	60	24	56
15	2-naphthyl	H	24	80	5	94
16	C ₆ H ₅	MeO	3	60	2	95
17	C ₆ H ₅	Me	16	60	2	93
18	C ₆ H ₅	F	20	60	2	67
19	cyclohexyl	H	26	60	3	88
20	<i>n</i> -heptyl	H	25	60	3	77

^a 0.5 mL of *tert*-amyl alcohol was used. ^b Isolated yields after purification by preparative thin-layer chromatography.

TABLE 5. Arylation of Aldehydes Using Dirhodium(II) Trifluoroacetate as the Catalyst^b


entry	Ar	product	T (°C)	time (h)	yield ^a (%)
1	2-naphthyl	24	60	5	93
2	2,6-Me ₂ C ₆ H ₃	17	60	1	79
3	<i>p</i> -CNC ₆ H ₄	21	60	4	60

^a 0.5 mL of *t*-amyl alcohol was used. ^b Isolated yields after purification by preparative thin-layer chromatography.

(Rh₂(tfa)₄) instead of Rh₂(pfb)₄, the alcohol **24** was obtained in 93% at 60 °C (Table 5, entry 1). This catalytic system was also more efficient in the arylation of bulky aldehyde 2,6-dimethylbenzaldehyde although the electron-deficient *p*-cyanobenzaldehyde afforded the alcohol in similar yield to that obtained when Rh₂(pfb)₄ was used (Table 5, entries 2 and 3).

We envisioned that the active catalyst would accommodate the NHC **4** coordination on the Rh(II) complex axial position, and we wished to provide structural evidence in support of this hypothesis. Consequently, and following a straightforward protocol in which the corresponding NHC was generated in situ in the presence of Rh₂(OAc)₄, we successfully prepared complexes **27** and **28** (72 and 60%, respectively) with NHCs attached on both axial positions (Figure 1).

The isolated bis-NHC complex **27** was tested as catalyst in the arylation of several aldehydes (Table 6). We were pleased to observe that the complex not only is a highly efficient catalyst for this transformation but also allowed a considerable reduction on the quantity of catalyst (1 mol % instead of 3 mol % used in the in situ method; see Table 2, entry 8) and base required.

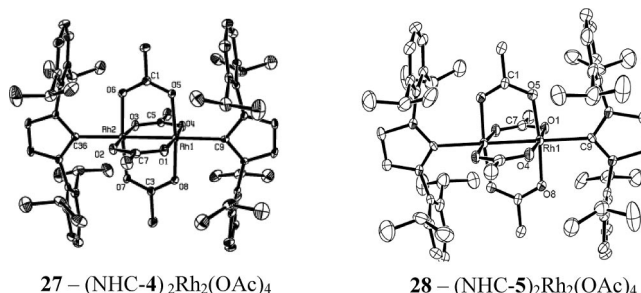
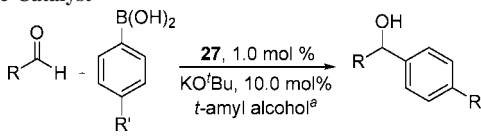


FIGURE 1. ORTEP¹¹ diagrams (ellipsoids at 30% probability) of the two di-Rh complexes.¹²

TABLE 6. Arylation of Aryl and Alkyl Aldehydes Using Complex **27** as the Catalyst^a


entry	R	R'	product	T (°C)	time (h)	yield ^b (%)
1	4-MeOC ₆ H ₄	H	3	90	1	87
2	(3,4-OCH ₂ O)C ₆ H ₃	H	29	90	3	96
3	4-CNC ₆ H ₄	H	21	90	6	78
4	C ₆ H ₅	MeO	3	90	1	95
5	C ₆ H ₅	Me	16	90	6	96
6	C ₆ H ₅	F	20	90	6	95
7	<i>n</i> -heptyl	H	25	90	6	99

^a 0.5 mL of *tert*-amyl alcohol was used. ^b Isolated yields after purification by preparative thin-layer chromatography.

When using complex **27**, the reaction proceeded considerably faster and in higher yields at higher temperatures; in fact, no reaction was observed at 60 °C. This observation can be rationalized by taking into account the fact that one of the NHC axial ligands must be displaced in order to leave one vacant axial coordination site on the dirhodium(II) complex. This supposition was corroborated by the fact that, from the reaction crude mixture in which complex **27** was successfully used as catalyst (yielding the alcohol **16** quantitatively) was isolated the complex with only one NHC **4** attached to the Rh₂(OAc)₄ moiety (75% of the initial quantity of complex **27** used). Most importantly, the isolated mono-NHC complex performed efficiently in the arylation of *p*-tolualdehyde, affording the alcohol **16** in 95% isolated yield. The same (NHC **4**)Rh₂(OAc)₄ species was identified by mass spectroscopy (MS *m/z* (rel intensity) = 830.11 (36)) of the crude mixture of the arylation reaction of aldehyde **1**. In addition, the complex possessing saturated NHC **5** ligands (SIPr) was tested in the same transformation. As expected, this complex afforded the alcohol **16** in 95% yield, although, to our delight, the monocomplex (NHC **5**)Rh₂(OAc)₄ was this time recovered from the reaction crude mixture in 97% yield.

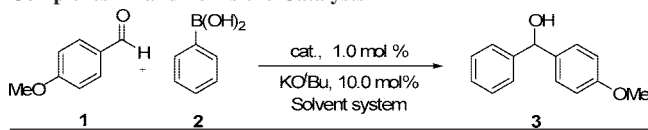
It was observed that complex **28** operates at even milder conditions than complex **27**. The latter afforded **3** only in 67% yield at 60 °C in methanol, whereas complex **28** successfully arylated the aldehyde in 94% yield (Table 7, entries 1 and 2).

The complex **28** proved to be an efficient catalyst for this transformation, allowing the efficient arylation of a series of aryl and alkyl aldehydes as shown in Table 8.

It was clearly of interest to attempt to isolate the mono-NHC complexes as it was anticipated that these would be active catalysts. Thus, these complexes were synthesized by simple eluting the parent bis-complexes on preparative thin-layer chromatography (PTLC). The characteristic red wine color of

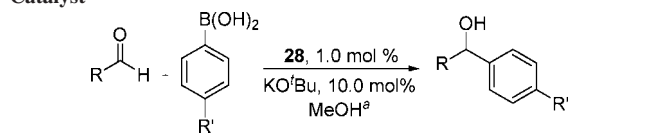
(11) Farrugia, L. ORTEP3 for Windows. *J. Appl. Crystallogr.* **1997**, *30*, 565.

(12) Deposited as CCDC deposit nos. 639254 and 644438 and published in ref 5.

TABLE 7. Solvent Effect over the Arylation of Aldehyde **1** Using Complexes **27** and **28** As the Catalysts


entry	catalyst	solvent system	<i>T</i> (°C)	time (h)	yield ^b (%)
1	27	MeOH	60	5.5	67
2	28	MeOH	60	5.5	94
3	28	DME/H ₂ O ^a	60	5.5	n.r.
4	28	DME/H ₂ O ^a	90	5.5	94

^a Organic solvent/H₂O (0.5:0.12 mL). ^b Isolated yields after purification by preparative thin-layer chromatography. n.r. = no reaction.

TABLE 8. Arylation of Aldehydes Using Complex **28** as the Catalyst^a


entry	R	R'	product	<i>T</i> (°C)	time (h)	yield ^b (%)
1	C ₆ H ₅	H	15	60	13	96
2	(3,4-OCH ₂ O)C ₆ H ₃	H	29	60	7	96
3	4-MeOC ₆ H ₄	H	3	60	6	94
3	4-CNC ₆ H ₄	H	21	reflux	17	95
4	<i>n</i> -heptyl	H	25	60	15	93
5	C ₆ H ₅	Me	16	60	13	99
6	C ₆ H ₅	F	20	60	16	99

^a 0.5 mL of MeOH was used. ^b Isolated yields after purification by preparative thin-layer chromatography (1/4 AcOEt/Hex).

the mono(NHC) complex appeared immediately as the bis-complex orange solution was applied in the PTLC. Suitable crystals for X-ray crystallography were obtained for both complexes allowing their structural elucidation (Figure 2).

A comparison of the structural similarity of the symmetrical complexes **27** and **28** with the unsymmetrical complexes **30** and **31** is of interest. Although there is an obvious change in the coordination geometry of the Rh₂ atoms, which is now a square-based pyramid, the remaining overall geometric parameters are similar. The Rh–Rh bonding distance and the Rh–C (carbene) distances are as expected slightly smaller and comparable to the values found in related compounds with a carboxylate cage structure.¹⁴

(13) Crystallographic data for complex **30**: C₄₉H₆₄N₂O₈Rh₂, FW = 1014.84, monoclinic, space group *P21/n*, *a* = 16.992(6) Å, *b* = 16.649(4) Å, *c* = 18.948(5) Å, α = 116.300(8)°, *V* = 4806(2) Å³, *Z* = 4, *T* = 150 K, ρ_{calc} = 1.403 mg·m⁻³, μ = 0.739 mm⁻¹, *F*(000) = 2104. Data were collected on a Bruker AXS-KAPPA APEX II diffractometer using graphite-monochromated Mo Kα radiation λ = 0.71069 Å, purple crystals (0.13 × 0.08 × 0.06 mm). Of 35575 reflections, 12008 were independent (*R*_{int} = 0.2299); 564 variables refined to final *R* indices *R*1 (*I* > 2σ(*I*)) = 0.0853, *wR*2(*I* > 2σ(*I*)) = 0.1521, *R*1(all data) = 0.2208, *wR*2(all data) = 0.2013, GoF = 0.870. Structure was solved by direct methods (SIR97). Non-hydrogen atoms were refined anisotropically, and hydrogen atoms were inserted in calculated positions, riding in the parent carbon atom (WINGX). CCDC deposit number 654664. Crystallographic data for complex **31**: C₂₅H₃₀N₂O₈Rh₂, FW = 832.59, orthorhombic, space group *P212121*, *a* = 12.659(4) Å, *b* = 15.502(2) Å, *c* = 18.822(3) Å, *V* = 3693.6(14) Å³, *Z* = 4, *T* = 150 K, ρ_{calc} = 1.497 mg·m⁻³, μ = 0.944 mm⁻¹, *F*(000) = 1712. Data were collected on a Bruker AXS-KAPPA APEX II diffractometer using graphite-monochromated Mo Kα radiation λ = 0.71069 Å, purple crystals (0.14 × 0.09 × 0.05 mm). Of 16605 reflections, 7325 were independent (*R*_{int} = 0.0588); 436 variables refined to final *R* indices *R*1(*I* > 2σ(*I*)) = 0.0422, *wR*2(*I* > 2σ(*I*)) = 0.0730, *R*1(all data) = 0.0591, *wR*2(all data) = 0.0779, GoF = 0.955. Structure was solved by direct methods (SIR97). Non-hydrogen atoms were refined anisotropically and hydrogen atoms were inserted in calculated positions, riding in the parent carbon atom. (WINGX) CCDC deposit nno. 654665.

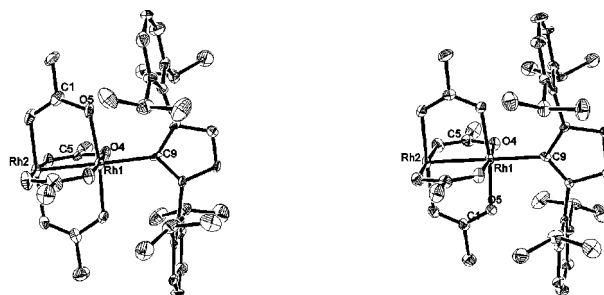
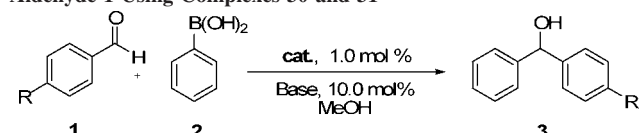
**30** – (NHC **4**)Rh₂(OAc)₄**31** – (NHC **5**)Rh₂(OAc)₄

FIGURE 2. ORTEP¹¹ diagrams (ellipsoids at 30% probability) of the two di-Rh complexes. Solvent molecules as well as hydrogen atoms were excluded for clarity. Selected bond lengths and angles for compounds **30** and **31**, respectively, are presented: Rh1–Rh2 = 2.417(1) Å, Rh1–C9 = 2.126(7) Å; Rh1–Rh2 = 2.426(6) Å, Rh1–C9 = 2.114(4) Å. All of the coordination angles are around 90°. ¹³

TABLE 9. Catalyst and Base Effect over the Arylation of Aldehyde **1** Using Complexes **30** and **31**


entry	R	complex	base	<i>T</i> (°C)	time (h)	yield ^b (%)
1	Me	30	KOtBu	60	3	75 ^a
2	Me	31	KOtBu	60	3	100 ^a
3	MeO	31		60	5	25 ^a
4	MeO	31	KOtBu	60	5	86
5	MeO	31	KOH	60	5	96

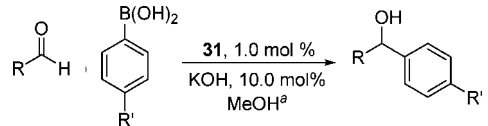
^a Conversion based on ¹H NMR. ^b Isolated yields after purification by preparative thin-layer chromatography.

The analogous complexes **27** and **28** exhibit different N–C–C–N torsion angles (0.20(2) and 8.35(2)°) and different N–C (1.388(4)/1.391(4) and 1.486(10)/1.469(10) Å) and C–C distances (1.343(4) and 1.495(12) Å), which we attribute to the differences between the saturated and unsaturated carbenes. These differences are also observed when comparing complexes **30** and **31**, where the N–C–C–N torsion angles (–1.62(9) and 12.15(5)°) and different N–C (1.382(9)/1.390(10) and 1.473(6)/1.470(6) Å) and C–C distances (1.332(14) and 1.513(12) Å).

Regarding the higher efficiency displayed by complex **31** in the arylation of **1** (Table 9, entries 1 and 2), the saturated monocomplex (NHC **5**)Rh₂(OAc)₄ **31** was further evaluated as a catalyst in this transformation. Surprisingly, complex **31** performed better when KOH was used as the base (Table 9, entries 2 and 3). The necessity of using a catalytic amount of base was clearly highlighted by the fact that in its absence only 25% of product was obtained (Table 9, entry 3).

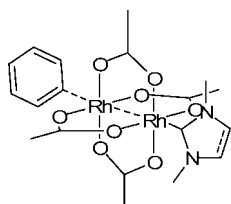
The optimized catalytic system was used in the arylation of a variety of aldehydes (Table 10). It is evident that complex **31** is superior to the bis-complex **28**, as reactions with **31** were run successfully at lower temperature (60 °C) and with reduced reaction times. Of particular note is the ability of complex **31** to promote reactions of alkyl aldehydes under considerable milder reaction conditions. The vinyl aldehydes tested afforded exclusively secondary alcohols **35** and **36**, and no 1,4-addition products were observed. Despite this enhanced reactivity and

(14) Snyder, J. P.; Padwa, A.; Stengel, T.; Arduengo III, A. J.; Jockisch, A.; Kim, H.-L. *J. Am. Chem. Soc.* **2001**, *123*, 11318–11319.

TABLE 10. Scope of the Methodology Using Complex **31** As the Catalyst^a


entry	R	R'	product	T (°C)	time (h)	yield ^b (%)
1	C ₆ H ₅	H	15	60	5	99
2	4-MeOC ₆ H ₄	H	3	60	5	96
3	4-CNC ₆ H ₄	H	21	reflux	5	97
4	C ₆ H ₅	Me	16	60	3.5	99
5	C ₆ H ₅	F	20	60	7	98
6	<i>n</i> -heptyl	H	25	60	1.5	98
7	cyclohexyl	H	26	60	1	94
8	Ph(CH ₂) ₂	H	32	60	1	94
9	PhCH ₂	H	33	60	2	90
10	<i>t</i> -Bu	H	34	60	1	60
11	<i>E</i> -PhCH(CH ₃)C	H	35	reflux	2	99
12	<i>trans</i> -PhCHCH	H	36	reflux	1.5	95

^a 0.5 mL of MeOH was used. ^b Isolated yields after purification by preparative thin-layer chromatography (1/4 AcOEt/Hex).

SCHEME 3. Envisioned Transmetalation Intermediate

selectivity it is gratifying to note that good functional group tolerance is retained.

Regarding the reaction mechanism, we envisioned the occurrence of a similar pathway to the one proposed by Hayashi et al. for the rhodium-catalyzed 1,4-addition of organoboronic acids, in which, transmetalation of the aryl group from boron to rhodium occurs (Scheme 3) followed by the addition to the aldehyde.¹⁵

Despite our attempts to obtain such transmetalation product directly from the reaction of monocomplexes **30** and **31** with phenylboronic acid, this phenylrhodium intermediate was never detected. Therefore, the method used by Hayashi et al. was attempted.^{15a} To our surprise the reaction of monocomplex **30** with phenyllithium in THF afforded the bis-complex **27** and the monocomplex **30** with a molecule of THF attach to the complex vacant coordination site (Scheme 4). Apart from dirhodium tetraacetate, no other dirhodium complex was detected in the reaction crude mixture.

DFT Calculations. The formation of bis-complex **27** is indicative of NHC dissociation from the monocomplex **30**. This

fact is probably related with the strong axial coordination of the phenyl group which weakens the NHC coordination sufficiently so that a molecule of THF is able to compete for the axial coordination site.

This possibility was tested with DFT calculations,¹⁷ used to optimize the geometry of a Rh₂(OAc)₄ complex with a phenyl group in an axial position. In the model used for calculations, the second axial position is occupied by NHC-7. This is the simplest NHC ligand studied with methyl as *N*-substituent and was chosen for computational expediency. The geometry obtained for [Rh₂(OAc)₄(NHC-7)(C₆H₅)]⁻ is represented in Figure 3, with the structure calculated for the mono-NHC complex, [Rh₂(OAc)₄(NHC-7)], for comparison purposes.

The main effect of axial coordination on the Rh₂(OAc)₄ core is a weakening of the Rh–Rh bond due to the population of a Rh–Rh antibonding orbital (σ^*) derived from the out-of-phase combination of Rh z^2 orbitals.⁵ Thus, the Rh–Rh bond length rises from 2.36 Å in bare [Rh₂(OAc)₄] to 2.44 Å in [Rh₂(OAc)₄(NHC 7)], following the coordination of one NHC ligand. Additional coordination of a phenyl group in the second axial position rises the Rh–Rh distance to 2.51 Å, in complex anion [Rh₂(OAc)₄(NHC)(C₆H₅)]⁻. The electronic reason underlying this trend is reflected by the corresponding Wiberg indices (WI)¹⁸ for the Rh–Rh bond, 0.78, 0.49, and 0.36, in the same order.

Of particular relevance is the influence of phenyl coordination on the Rh–NHC bond. This bond is severely weakened in the phenyl complex, when compared with the mono-NHC complex (see Figure 3 for relevant distances and Wiberg indices). The mutual influence of the two axial ligands in Rh₂(OAc)₄ complexes will be further addressed below, discussing borate complex **A**. The weakening of the Rh–NHC bond in the phenyl complex corroborates the experimental observations discussed above and, at the same time, discards the possibility of formation of a phenylrhodium intermediate in the reaction conditions. Therefore, we rationalized that the catalyst would be involved in the activation of the boronic acid, rather than in a transmetalation event, favoring in this way the direct transference of the phenyl group from the boron to the aldehyde. This direct transference is not an unknown process in the literature; in fact, it is the key step of the Petasis reaction in which the boronic acid acts as a nucleophile after reaction with an electron donor group forming an “ate” complex. The “ate” complex is inert to the carbonyl group but efficiently traps the C=N double bond (Scheme 5).¹⁹

Interestingly, the boronic acid moiety appears to be fundamental for the success of the catalytic process. When we tested the boronate ester, almost no arylation product was obtained (Scheme 6), the secondary alcohol formed was most likely due to the hydrolysis of the ester by traces of water present in the reaction conditions.

This result corroborated the importance of the boronic acid moiety and its putative coordination onto the dirhodium moiety. Therefore we investigated, using DFT calculations, the hypothesis of direct arylation of aldehydes assisted by a mono-NHC/Rh₂(OAc)₄ complex.

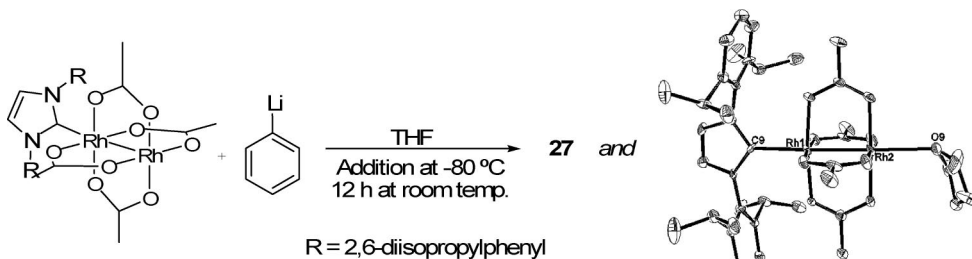
(17) Parr, R. G.; Yang, W. *Density Functional Theory of Atoms and Molecules*; Oxford University Press: New York, 1989.

(18) (a) Wiberg, K. B. *Tetrahedron* **1968**, *24*, 1083. (b) Wiberg indices are electronic parameters related to the electron density between atoms. They can be obtained from a Natural Population Analysis and provide an indication of the bond strength.

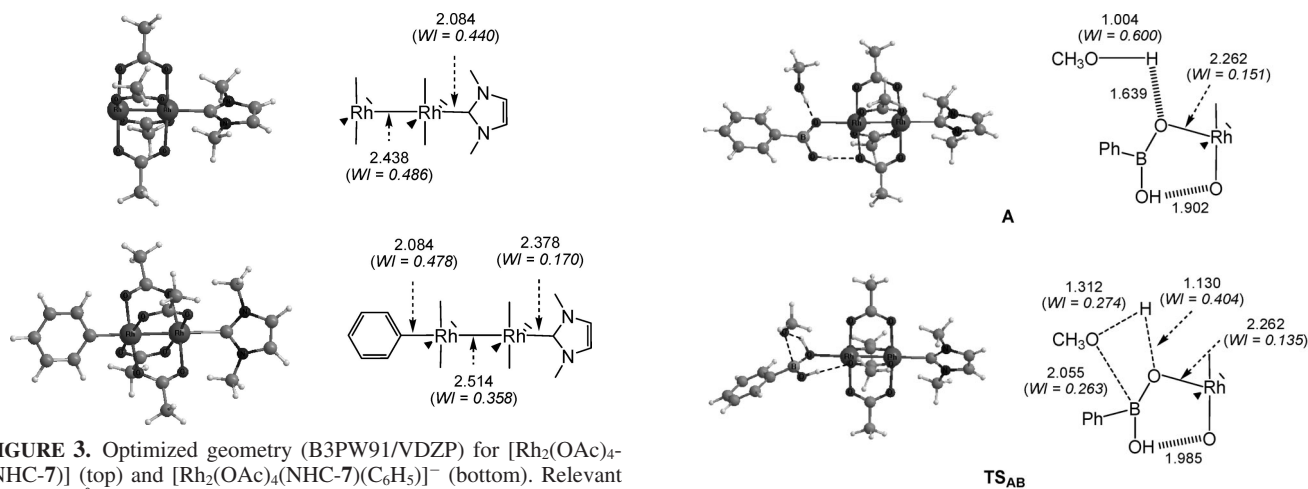
(19) Kaiser, P. F.; Churches, Q. I.; Hutton, C. A. *Aust. J. Chem.* **2007**, *60*, 799–810.

(15) (a) Hayashi, T.; Takahashi, M.; Takaya, Y.; Ogasawara, M. *J. Am. Chem. Soc.* **2002**, *124*, 5052–5058. (b) Kina, A.; Iwamura, H.; Hayashi, T. *J. Am. Chem. Soc.* **2006**, *128*, 3904–3905. (c) Kina, A.; Yasuhara, Y.; Nishimura, T.; Iwamura, H.; Hayashi, T. *Chem. Asian J.* **2006**, *1*, 707–711.

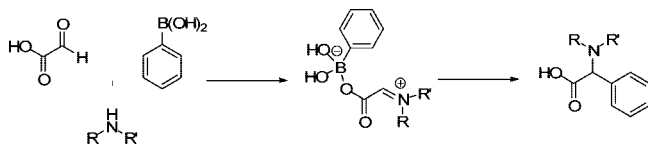
(16) Crystallographic data for complex CCDC 673880: C₃₀H₅₆N₂O₉Rh₂, FW = 902.68, monoclinic, space group *P21/c*, *a* = 17.537(8) Å, *b* = 12.284(7) Å, *c* = 19.233(7) Å, α = 105.540(2)°, *V* = 3992(3) Å³, *Z* = 4, *T* = 150 K, ρ_{calc} = 1.502 mg·m⁻³, μ = 0.881 mm⁻¹, *F*(000) = 1864. Data were collected on a Bruker AXS-KAPPA APEX II diffractometer using graphite-monochromated Mo K α radiation λ = 0.71069 Å, purple crystals (0.10 × 0.06 × 0.02 mm). Of 37555 reflections, 7247 were independent (*R*_{int} = 0.2259); 481 variables refined to final *R* indices *R*1(*I* > 2 σ (*I*)) = 0.0647, *wR*2(*I* > 2 σ (*I*)) = 0.0963, *R*1(all data) = 0.1715, *wR*2(all data) = 0.1186, *GoF* = 0.887. Structure was solved by direct methods (SIR 2004). Non-hydrogen atoms were refined anisotropically, and hydrogen atoms were inserted in calculated positions, riding in the parent carbon atom. (WINGX) CCDC deposit no. CCDC 673880.

SCHEME 4. Reaction of Monocomplex 30 with PhLi^a 

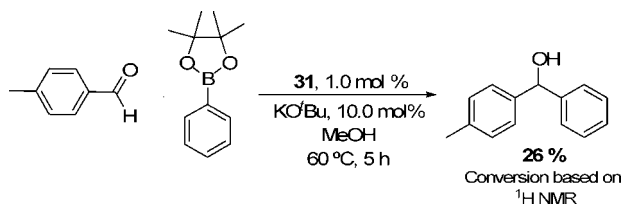
^a ORTEP diagrams (ellipsoids at 30% probability). Hydrogen atoms were excluded for clarity. Selected bond lengths and angles: $\text{Rh1-Rh2} = 2.4204(11)$ Å, $\text{Rh1-C9} = 2.181(7)$ Å, $\text{Rh2-O9} = 2.462(6)$ Å. All of the coordination angles are around 90° .¹⁶



SCHEME 5. Petasis Reaction

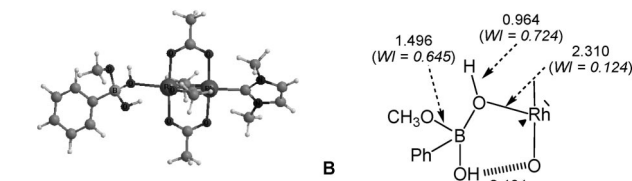


SCHEME 6. Arylation of Aldehydes with Boronic Esters



In a preliminary mechanistic study we started with the complex $[\text{Rh}_2(\text{OAc})_4(\text{NHC-7})(\text{BPh}(\text{OH})\text{O})]^-$ with borate, $\text{BPh}(\text{O}-\text{H})\text{O}^-$, occupying the second axial position, taken as the initial reactant of the catalytic cycle.²⁰ In this species, **A**, one solvent molecule (CH_3OH) is considered explicitly. The geometry optimized for **A** is depicted in Figure 4.

In **A**, phenyl borate ($\text{BPh}(\text{OH})\text{O}^-$) coordinates the Rh_2 unit, occupying one axial position. The corresponding $\text{Rh}-\text{O}$ bond is well established with a bond distance of 2.26 Å and a Wiberg index of 0.15 . The $\text{Rh}-\text{NHC}$ bond is longer (2.20 Å) and weaker ($\text{WI} = 0.26$) than the one existing in the mono-NHC complex, $[\text{Rh}_2(\text{OAc})_4(\text{NHC-7})]$ (see Figure 3). Similar to what happened in the phenyl complex, borate coordination pushes



the NHC away from the metal fragment. The reason for the weakening of the $\text{Rh}-\text{NHC}$ bond in **A**, when compared with the mono-NHC complex, can be traced to the electronic structure of the borate complex and, in particular, to the charge distribution among the different fragments, obtained by means of a natural population analysis (NPA).²¹ The charge of the central fragment, $\text{Rh}_2(\text{OAc})_4$, is practically the same in **A** (-0.30) and in the mono-NHC complex (-0.33), while the NHC is considerably less positive in **A** than in $[\text{Rh}_2(\text{OAc})_4(\text{NHC-7})]$ (with charges of 0.15 and 0.33 , respectively). Thus, the NHC ligand acts as an electron buffer in **A**, releasing excess electron density on the $\text{Rh}_2(\text{OAc})_4$ core due to coordination of the second

(20) Recently, Hartwig et al. reported Rh(I) arylboronate complexes. Zhao, P.; Incarvito, C. D.; Hartwig, J. F. *J. Am. Chem. Soc.* **2007**, *129*, 1876–1877.

(21) (a) Carpenter, J. E.; Weinhold, F. J. *THEOCHEM* **1988**, *169*, 41. (b) Carpenter, J. E. Ph.D. thesis, University of Wisconsin, Madison, WI, 1987. (c) Foster, J. P.; Weinhold, F. *J. Am. Chem. Soc.* **1980**, *102*, 7211. (d) Reed, A. E.; Weinhold, F. *J. Chem. Phys.* **1983**, *78*, 4066. (e) Reed, A. E.; Weinhold, F. *J. Chem. Phys.* **1983**, *78*, 1736. (f) Reed, A. E.; Weinstock, R. B.; Weinhold, F. *J. Chem. Phys.* **1985**, *83*, 735. (g) Reed, A. E.; Curtiss, L. A.; Weinhold, F. *Chem. Rev.* **1988**, *88*, 899. (h) Weinhold, F.; Carpenter, J. E. *The Structure of Small Molecules and Ions*; Plenum: New York, 1988; p 227.

axial ligand. This electron flow between axial ligands, in a tandem effect, allows coordination of the second axial ligand with minimal changes on the electron density of the metal fragment. In the case of a very strong donor, such as phenyl, the Rh–NHC bond is severely weakened, and this ligand can be expelled under the experimental conditions.

Phenyl borate coordination in **A** is reinforced by one hydrogen interaction between the OH bond of borate and one O-atom of a bridging acetate with a OH–O distance of 1.90 Å and a O–H–O angle of 166°. Similarly, the methanol molecule establishes one hydrogen bond with the coordinated O-atom of borate with an OH–O distance of 1.64 Å and an O–H–O angle of 175°.

Attack of the methanol molecule upon coordinated borate yields an “ate” complex with tetravalent boron (**B**). The new boron ligand, BPh(MeO)(OH)₂[−], coordinates the metal through one OH arm (Figure 4) with a Rh–O bond slightly longer (2.31 Å) and weaker (WI = 0.12) than the one existing in **A**. As a consequence, the Rh–NHC bond in **B** is shorter (2.18 Å) and stronger (WI = 0.28) than the one existing in **A**, revealing, once more, the electronic communication between axial ligands. Interestingly, coordination of the boron tetravalent ligand in **B**, is reinforced by one hydrogen interaction between the uncoordinated OH arm in the ligand, and the O-atom of a bridging acetate in the metal fragment, having an OH–O distance of 2.10 Å and an O–H–O angle of 162°.

The first step of the reaction, from **A** to **B**, corresponds to addition of the O–H bond of methanol to the B–O bond of coordinated borate in **A**. In the transition state associated with this process (**TS_{AB}**, Figure 4), O–H bond breaking in the methanol molecule is well advanced with a rather long distance (1.31 Å) corresponding to a weak interaction (WI = 0.27), compared with the methanol molecule in **A** ($d_{\text{O-H}} = 1.00$ Å, WI = 0.60). On the other hand, the new B–O bond is starting to form in **TS_{AB}** with a bond distance of 2.06 Å and a Wiberg index of 0.26, the same happening with the new O–H bond ($d_{\text{O-H}} = 1.13$ Å, WI = 0.40). For comparison purposes, the corresponding values in **B**, where these two bonds are completely established, are 1.50 Å and WI = 0.64, for B–O, and 0.96 Å and WI = 0.72, for O–H. Interestingly, the Rh–O bond existing in **TS_{AB}** ($d_{\text{Rh-O}} = 2.26$ Å, WI = 0.13) is essentially equivalent to the one observed in the borate complex, **A**, showing that borate coordination is maintained along the process of methanol addition and formation of the “ate” complex. Moreover, coordination of the boron moiety in **TS_{AB}** is supported by an H-bond between one OH arm in the ligand and one O-atom of a bridging acetate ligand ($d_{\text{OH-O}} = 1.98$ Å, O–H–O = 164°), similar to what is observed in the minima **A** and **B**.

Formation of the “ate” complex **B** from the borate species (**A**) and one solvent molecule is a slightly exergonic process ($\Delta G = -1.2$ kcal/mol) with an accessible energy barrier of 21.9 kcal/mol. The calculated energy profile is represented in Figure 5.

Once activation of the boronic acid is achieved, through formation of the “ate” complex, **B**, the mechanism of the reaction of aldehyde arylation was further investigated using acetaldehyde as model reactant. The initial species in the phenylation step (**C**) corresponds to an aggregate of the “ate” complex **B** and one molecule of acetaldehyde. Its optimized structure is represented in Figure 6.

In **C**, the structure of the “ate” complex **B** is retained despite the presence of the neighbor acetaldehyde molecule, with maximum deviations of 0.006 Å in the coordination

distances and of 0.004 in the corresponding Wiberg indices, comparing **B** and **C**. The aldehyde molecule binds the complex through two hydrogen bonds. One is established between the carbonyl hydrogen atom in acetaldehyde and the O-atom in the MeO arm of the tetravalent boron ligand ($d_{\text{CH-O}} = 2.04$ Å, C–H–O = 156°).²² The other H-interaction connecting the aldehyde molecule and the “ate” complex involves the oxygen atom on the aldehyde and hydrogen atom in the coordinated OH arm of the boron ligand ($d_{\text{OH-O}} = 2.23$ Å, C–H–O = 160°). Formation of the aggregate of the “ate” complex with one aldehyde molecule (in **C**), from the bare complex (**B**), is a slightly endergonic process with $\Delta G = 2.9$ kcal/mol (see Figure 5).

Phenyl addition to the carbonyl C-atom of the aldehyde in **C** produces species **D**. The product **D** corresponds to a methyl borate complex with one hydrogen-bonded phenylmethanol molecule. This species is related to the initial reagent considered, complex **A**. Both are complexes with a borate ligand in one axial position: phenyl borate in **A** and methyl borate in **D**. Moreover, in both species there is one alcohol molecule connected to the complex by means of hydrogen bonds: one solvent molecule (methanol) in **A** and the product alcohol (phenylmethanol) in **D**. Accordingly, bonding is essentially equal in both species (**A** and **D**) with coordination distances within 0.02 Å and Wiberg indices within 0.004. In **D**, such as in **A**, borate coordination is reinforced through a H-bond between the OH arm of that ligand and one O-atom of a bridging acetate ($d_{\text{OH-O}} = 1.94$ Å, C–H–O = 166°). The establishment of a hydrogen bond between the phenylmethanol molecule, that is, the reaction product, and the complex core is reflected in a distance of 1.57 Å between the OH group of the alcohol and the O[−] arm in the borate ligand (O–H–O = 173°).

The reaction of phenylation of the acetaldehyde molecule, that is, from **C** to **D**, corresponds to the transfer of the phenyl group from boron to the C-atom of the carbonyl group in aldehyde, while, at the same time, one hydrogen atom is shifted from the coordinated OH bond (in **C**) to the O-atom of the aldehyde. This process occurs in a single step and, in the corresponding transition state (**TS_{CD}**, Figure 6), the reactants are connected through a 6-member ring: BCCOHO. **TS_{CD}** is a rather early transition state, since both the new bonds, C(Ph)–C(C=O) and H(OH)–O(C=O), are only incipient, and the process of B–C(Ph) and H–O bond breaking is only beginning (see Figure 6 for relevant distances and Wiberg indices). Coordination of the boron ligand is maintained along the process, as revealed by a Rh–O distance of 2.31 Å and a Wiberg index of 0.10, in **TS_{CD}**, as well as by the H-bond between the boron ligand and the bridging acetate, such as in **C** and in **D** ($d_{\text{OH-O}} = 2.01$ Å, C–H–O = 162°).

The phenylation step, from **C** to **D**, has an energy barrier of 25.8 kcal/mol (Figure 5) being, thus, slightly higher than the one corresponding to the first step, i.e., formation of the “ate” complex, from **A** to **B**. However, the entire process, corresponding to the formation of one phenylmethanol molecule, from **A** to **D**, is rather favorable, from the thermodynamic point of view, with $\Delta G = -31.7$ kcal/mol.

To close the catalytic cycle, **A** has to be regenerated from **D**. That corresponds to exchange borate ligands and alcohol molecules from methyl borate and phenylmethanol, in **D**, back to phenyl borate and methanol, in **A**. In this process two fresh molecules of reagents, phenylboronic acid and solvent (methanol), are consumed, while one molecule of the reaction

(22) Corey, E. J.; Lee, T. W. *Chem. Commun.* **2001**, 1321, 1329.

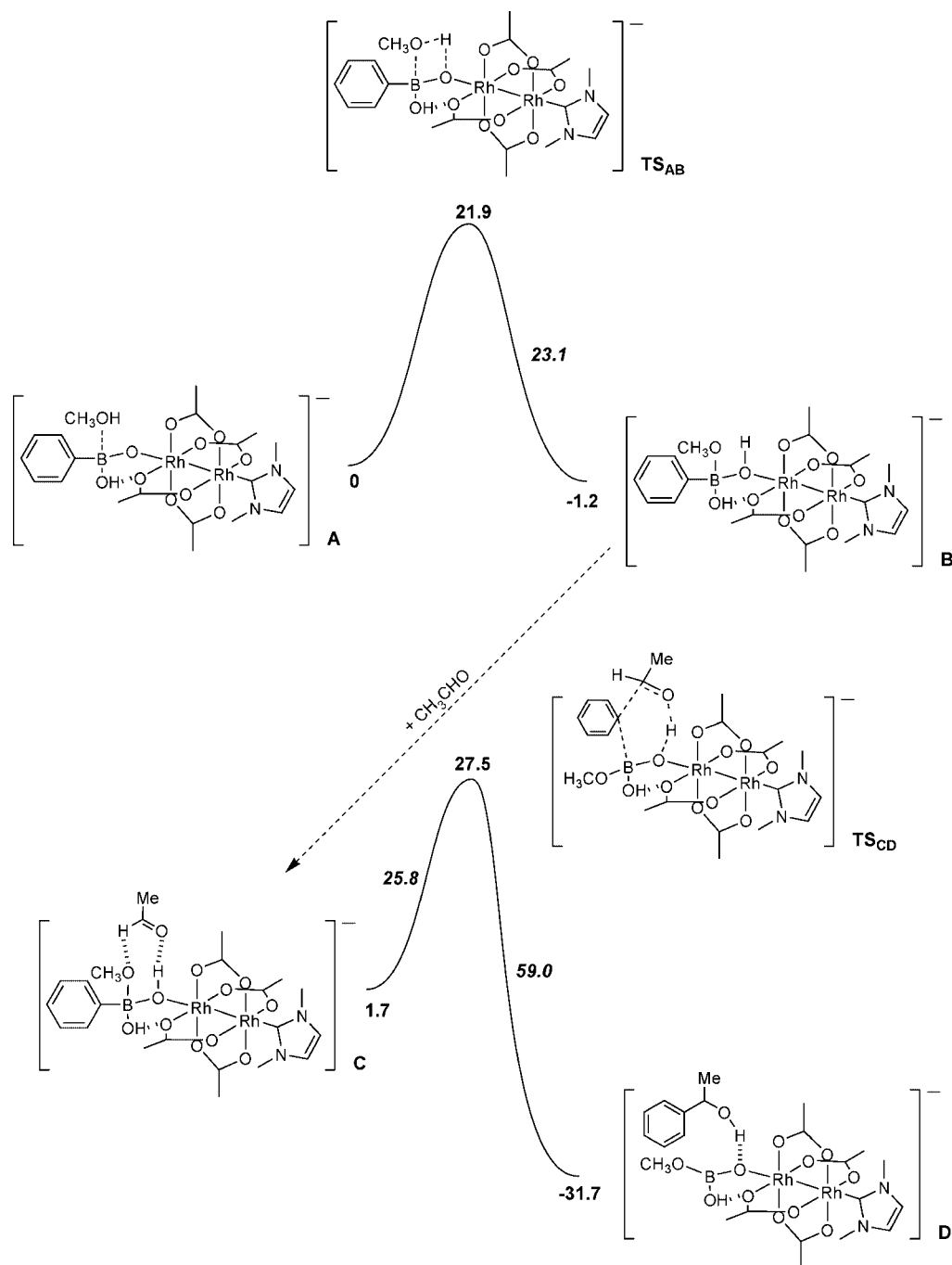


FIGURE 5. Energy profile (kcal/mol) calculated (B3PW91/VDZP) for the phenylation of acetaldehyde in methanol, starting with borate complex A. Energy barriers are presented in italics.

product, phenylmethanol, and one molecule of methylboronic acid (a side product) are released. The overall energy balance for regeneration of **A** from **D** is $\Delta G = -4.5$ kcal/mol (Scheme 7), and thus, closure of the catalytic cycle is a favorable process, from thermodynamic point of view.

In summary, results from a preliminary DFT mechanistic investigation indicate that the role of the $\text{Rh}_2(\text{OAc})_4$ catalyst is centered on the activation of the phenylboronic acid, through formation of an “ate” complex with tetravalent boron. Phenyl transfer would, then, follow the formation of this “ate” complex. In addition, the reaction of phenylation occurs without direct metal participation and, in particular, without aldehyde coordination. Most importantly, hydrogen bonding is present along

the entire mechanism, being essential in the definition of the relative orientation of reactants in each step, as well as in supporting the coordination of boron ligands to the metal fragment. This result can explain the absence of significant reaction experimentally observed when boronate esters are used instead of boronic acid (see above). In fact, without the OH groups, existing in the acid but not in the esters, it is not possible the establishment of H-bonds between the boron reagent and the metallic moiety $[\text{Rh}_2(\text{OAc})_4]$.

It should be noticed that given the nature of the solvent experimentally employed (alcohol), the explicit consideration of only one solvent molecule in the calculations may lead to a poor description of the system, despite the correction of the

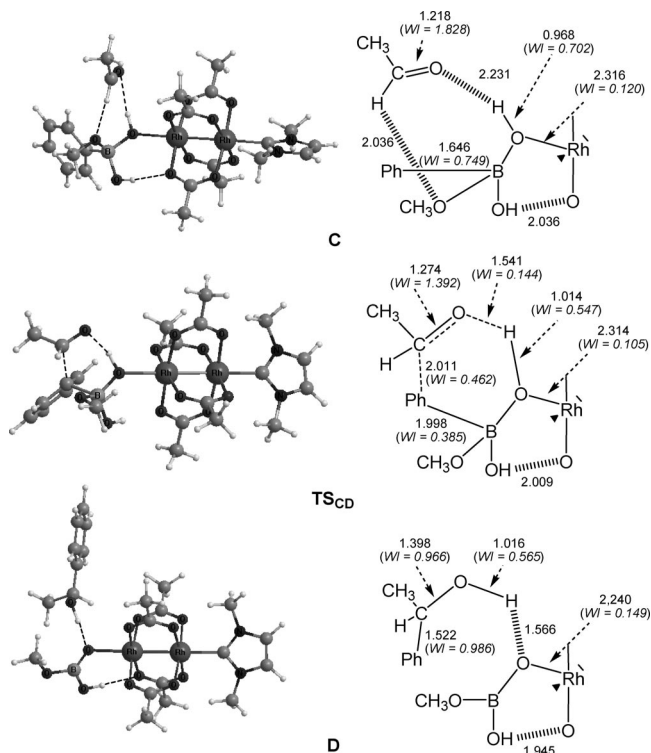
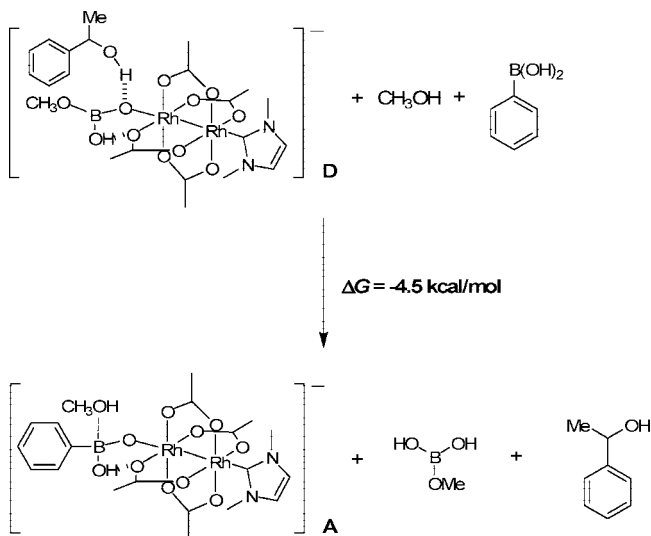


FIGURE 6. Optimized geometry (B3PW91/VDZP) for the “ate” complex with an acetone molecule **C** (top), the product of aldehyde phenylation: a methyl-borate complex H-bonded with one molecule of phenylmethanol **D** (bottom), and the corresponding transition state (**TS_{CD}**, center). Relevant distances (Å) and Wiberg indices (WI, italics) are indicated.

SCHEME 7. Energy Balance for Regeneration of the Borate Complex **a** and Closing of the Catalytic Cycle



energy values with a polarizable continuum model (see Computational Details). Thus, the results from the DFT mechanistic investigations should be taken with due caution.

Summary

We have disclosed a highly efficient new methodology for the arylation of aryl, alkyl and vinyl aldehydes using arylboronic acids as the aryl transfer agent. The results obtained taken together with theoretical and structural studies performed on

this system, have unveiled a new reaction mode for dirhodium complexes. If our model is correct, it establishes NHCs **4** and **5** as preferential axial ligands which confer high steric protection around one of the Rh atoms stabilizing the catalyst effectively tuning the reactivity of this well-known class of catalysts. The experimental and structural work highlighted the saturated mono species ((NHC-**5**)Rh₂(OAc)₄) as the most active catalyst. DFT calculations indicate that hydrogen bonding and solvent participation play a fundamental role in the reaction mechanism. Further experimental and computational studies will be conducted in order to extend the scope of the methodology and to fully understand the reaction mechanism.

Experimental Section

General Information. Tetrahydrofuran (THF), dichloromethane (DCM), 1,2-dimethoxyethane (DME), acetonitrile (CH₃CN), toluene, and *tert*-amyl alcohol were freshly distilled over calcium hydride prior to use. Ethyl acetate was distilled over potassium carbonate, while methanol was distilled from magnesium. All reactions were performed in oven-dried glassware under dry argon atmosphere. Flash chromatography was carried out on silica gel 60 M purchased from MN (ref 815381), preparative thin-layer chromatography plates were prepared with silica gel 60 GF₂₅₄ Merck (ref 1.07730.1000). Reaction mixtures were analyzed by TLC using ALUGRAM SIL G/UV₂₅₄ from MN (ref 818133, silica gel 60), and visualization of TLC spots was effected using UV and phosphomolybdic acid solution. NMR spectra were recorded using CDCl₃ as solvent and (CH₃)₄Si (¹H) as internal standard. All coupling constants are expressed in Hz. Dirhodium catalysts were purchased from a commercial supplier: Rh₂(OAc)₄, rhodium(II) acetate dimer; Rh₂(pfb)₄, rhodium(II) heptafluorobutyrate dimer; Rh₂(Ooct)₄, rhodium(II) octanoate dimer. Dirhodium(II) caprolactam (Rh₂(cap)₄) was prepared according to literature procedures (see the Supporting Information). NHC ligands used were prepared following reported procedures: 1,3-bis(*tert*-butyl)imidazolium chloride, 1,3-bis(*tert*-butyl)imidazolium chloride, 1,3-bis(2,6-diisopropylphenyl)imidazolium chloride and 1,3-bis(2,6-diisopropylphenyl)imidazolium chloride, were prepared according to literature procedures (see Supporting Information), except 1,3-bis(2,4,6-trimethylphenyl)imidazolium chloride which was purchased from a commercial supplier. 1,3-Dimethylimidazolium iodide was prepared by simple alkylation of 1-methylimidazole with iodomethane in toluene at room temperature for 2 h (99% yield). The aldehydes and boronic acids were purchased from a commercial supplier and used without further purification.

Synthesis of Complex 30. Complex **27** (0.021 g, 1.72 × 10⁻² mmol) was eluted by preparative thin-layer chromatography (30% ethyl acetate in hexanes) yielding the respective monocomplex, Rh₂(OAc)₄-*i*-PrNHC**30** (0.012 g, 90% yield). The monocomplex formation was observed by an immediate change of color from orange to red wine color in the plate. Further recrystallizations from toluene afforded purple crystals suitable for X-ray crystallography: ¹H NMR (C₇D₈) δ (ppm) = 7.09–6.97 (m, toluene), 6.60 (s, 2H), 4.28 (s), 3.27–3.24 (m, 4H), 2.11–2.07 (toluene), 1.31 (s, 12H), 1.18 (d, 12H, *J* = 9.2 Hz), 1.06 (d, 12H, *J* = 9.0 Hz); ¹³C NMR (C₇D₈) δ (ppm) = 188.20, 145.61, 122.79, 28.10, 25.06, 22.83, 22.60. Anal. Calcd for C₃₅H₄₈N₂O₈Rh₂: C, 50.61; H, 5.83; N, 3.37. Found: C, 49.65; H, 6.03; N, 3.10. Additional NMR experiments such as DEPT and HMQC were carried out and confirmed the characterization described.

Synthesis of Complex 31. Complex **28** (0.021 g, 1.72 × 10⁻² mmol) was eluted by preparative thin-layer chromatography (30% ethyl acetate in hexanes) yielding the respective monocomplex, Rh₂(OAc)₄-*S*-*i*-PrNHC**31** (0.013 g, 98% yield). The monocomplex formation was observed by an immediate change of color from orange to red wine color in the plate. Further recrystallizations from toluene afforded purple crystals suitable for X-ray crystallography: MS (FAB⁺) *m/z* = 832.0, 391.2; HMRS (FAB⁺) *m/z* calcd. 832.167723, found 832.169467; ¹H NMR (C₇D₈) δ (ppm) =

7.09–6.97 (m, toluene), 3.81 (s, 2H), 3.72–3–69 (m, 8H), 2.09–2.08 (toluene), 1.32–1.30 (m, 24H), 1.09 (d, 12H); ^{13}C NMR (C_7D_8) δ (ppm) = 188.29, 145.98, 139.02, 123.43, 54.40, 28.07, 25.31, 24.13. Anal. Calcd for $\text{C}_{35}\text{H}_{50}\text{N}_2\text{O}_8\text{Rh}_2$: C, 50.49; H, 6.05; N, 3.36. Found: C, 50.51; H, 6.47; N, 3.39. Additional NMR experiments such as HMQC were carried out and confirmed the characterization described.

General Procedure for the Evaluation of the in Situ Methodology (Table 4). $\text{Rh}_2(\text{pfb})_4$ (7.90 mg, 7.50×10^{-3} mmol, 3 mol %) was weighed into a flame-dried round-bottom flask equipped with a condenser and under argon atmosphere. *tert*-Amyl alcohol (0.5 mL) was added, the suspension was stirred at room temperature for 5 min, and then phenylboronic acid (61.00 mg, 0.50 mmol), 1,3-bis(2,6-diisopropylphenyl)imidazolium chloride (3.20 mg, 7.50×10^{-3} mmol, 3 mol %), KO^tBu (28.00 mg, 0.25 mmol), and the corresponding aldehyde (0.25 mmol) were successively added. The resulting mixture was stirred at 40, 60 or 80 °C for different periods of time. The reaction mixture was concentrated under reduced pressure and the residue was purified by preparative thin-layer chromatography (ethyl acetate/hexane) to yield the desired secondary alcohols.

General procedure for the Arylation of Aldehydes Using Complex 27 as the Catalyst (Table 6). Complex 27 (3.00 mg, 2.50×10^{-3} mmol, 1 mol %) was weighed into a flame-dried round-bottom flask equipped with a condenser and under argon atmosphere. *tert*-Amyl alcohol (0.5 mL), phenylboronic acid (61.00 mg, 0.50 mmol), and KO^tBu (2.80 mg, 0.025 mmol, 10 mol %) were successively added, and the resulting suspension was stirred at room temperature for 15 min after which the corresponding aldehyde (0.25 mmol) were added. The resulting mixture was stirred at 90 °C for different periods of time. The reaction mixture was concentrated under reduced pressure, and the residue was purified by preparative thin-layer chromatography (ethyl acetate/hexane) to yield the desired secondary alcohols.

General Procedure for the Arylation of Aldehydes Using Complex 28 as the Catalyst (Table 8). Complex 28 (3.00 mg, 2.50×10^{-3} mmol, 1 mol %) was weighed into a flame-dried round-bottom flask equipped with a condenser and under argon atmosphere. Methanol (0.5 mL), phenylboronic acid (61.00 mg, 0.50 mmol), and KO^tBu (2.80 mg, 0.025 mmol, 10 mol %) were successively added, and the resulting suspension was stirred at room temperature for 15 min after which the corresponding aldehyde (0.25 mmol) were added. The resulting mixture was stirred at 60 °C or reflux for different periods of time. The reaction mixture was concentrated under reduced pressure, and the residue was purified by preparative thin-layer chromatography (ethyl acetate/hexane) to yield the desired secondaries.

General Procedure for the Arylation of Aldehydes Using Complex 31 as the Catalyst (Table 10). Complex 31 (2.00 mg, 2.50×10^{-3} mmol, 1 mol %) was weighed into a flame-dried round-bottom flask equipped with a condenser and under argon atmosphere. Methanol (0.5 mL), phenylboronic acid (61.00 mg, 0.50 mmol), and KOH (1.40 mg, 0.025 mmol, 10 mol %) were successively added, and the resulting suspension was stirred at room

temperature for 15 min after which the corresponding aldehyde (0.25 mmol) were added. The resulting mixture was stirred at 60 °C or reflux for different periods of time. The reaction mixture was concentrated under reduced pressure, and the residue was purified by preparative thin-layer chromatography (ethyl acetate/hexane) to yield the desired secondary alcohols.

Computational Details. All calculations were performed using the Gaussian 03 software package,²³ and the B3PW91 hybrid functional, without symmetry constraints. That functional includes a mixture of Hartree–Fock²⁴ exchange with DFT¹⁷ exchange–correlation, given by Becke’s three-parameter functional²⁵ with Perdew and Wang’s 1991 gradient-corrected correlation functional.²⁶ The LanL2DZ basis set²⁷ augmented with an *f*-polarization function²⁸ was used for Rh and a standard 6-31G(d,p)²⁹ for the remaining elements. Transition-state optimizations were performed with the synchronous transit-guided quasi-newton method (STQN) developed by Schlegel et al.³⁰ Frequency calculations were performed to confirm the nature of the stationary points, yielding one imaginary frequency for the transition states and none for the minima. Each transition state was further confirmed by following its vibrational mode downhill on both sides and obtaining the minima presented on the energy profiles. A natural population analysis (NPA)²¹ and the resulting Wiberg indices¹⁸ were used for a detailed study of the electronic structure and bonding of the optimized species. Energy values reported along the text result from single point energy calculations with the solvent (methanol) effect taken into account through the polarizable continuum model (PCM) initially devised by Tomasi and co-workers³¹ as implemented on Gaussian 03³² and, thus, can be taken as free energy.³³ The molecular cavity was based on the united atom topological model applied on UAHF radii, optimized for the HF/6-31G(d) level.

Acknowledgment. We thank the Fundação para a Ciência e Tecnologia (POCI 2010) and FEDER (PTDC/QUI/66695/2006, PTDC/QUI/66015/2006, POCI/QUI/60175/2004, POCI/QUI/58791/2004, SFRH/BPD/18624/2004, and SFRH/BD/30619/2006) for financial support.

Supporting Information Available: Tables with atomic coordinates for all optimized species. This material is available free of charge via the Internet at <http://pubs.acs.org>.

JO800087N

(23) Becke, A. D. *J. Chem. Phys.* **1993**, *98*, 5648.

(26) (a) Burke, K.; Perdew, J. P.; Wang, Y. In *Electronic Density Functional Theory: Recent Progress and New Directions*; Dobson, J. F., Vignale, G., Das, M. P., Eds.; Plenum: New York, 1998. (b) Perdew, J. P. In *Electronic Structure of Solids '91*, Ed. Ziesche, P., Eschrig, H., Eds.; Akademie Verlag: Berlin, 1991; p 11. (c) Perdew, J. P.; Chevary, J. A.; Vosko, S. H.; Jackson, K. A.; Pederson, M. R.; Singh, D. J.; Fiolhais, C. *Phys. Rev. B* **1992**, *46*, 6671. (d) Perdew, J. P.; Chevary, J. A.; Vosko, S. H.; Jackson, K. A.; Pederson, M. R.; Singh, D. J.; Fiolhais, C. *Phys. Rev. B* **1993**, *48*, 4978. (e) Perdew, J. P.; Burke, K.; Wang, Y. *Phys. Rev. B* **1996**, *54*, 16533.

(27) (a) Dunning, T. H., Jr.; Hay, P. J. In *Modern Theoretical Chemistry*; Schaefer, H. F., III, Ed.; Plenum: New York, 1976; Vol. 3, p 1. (b) Hay, P. J.; Wadt, W. R. *J. Chem. Phys.* **1985**, *82*, 270. (c) Wadt, W. R.; Hay, P. J. *J. Chem. Phys.* **1985**, *82*, 284. (d) Hay, P. J.; Wadt, W. R. *J. Chem. Phys.* **1985**, *82*, 2299.

(28) Ehlers, A. W.; Böhme, M.; Dapprich, S.; Gobbi, A.; Höllwarth, A.; Jonas, V.; Köhler, K. F.; Stegmann, R.; Veldkamp, A.; Frenking, G. *Chem. Phys. Lett.* **1993**, *208*, 111.

(29) (a) Ditchfield, R.; Hehre, W. J.; Pople, J. A. *J. Chem. Phys.* **1971**, *54*, 724. (b) Hehre, W. J.; Ditchfield, R.; Pople, J. A. *J. Chem. Phys.* **1972**, *56*, 2257. (c) Hariharan, P. C.; Pople, J. A. *Mol. Phys.* **1974**, *27*, 209. (d) Gordon, M. S. *Chem. Phys. Lett.* **1980**, *76*, 163. (e) Hariharan, P. C.; Pople, J. A. *Theor. Chim. Acta* **1973**, *28*, 213.

(30) (a) Peng, C.; Ayala, P. Y.; Schlegel, H. B.; Frisch, M. J. *Comput. Chem.* **1996**, *17*, 49. (b) Peng, C.; Schlegel, H. B. *Isr. J. Chem.* **1994**, *33*, 449.

(31) (a) Cancès, M. T.; Mennucci, B.; Tomasi, J. *J. Chem. Phys.* **1997**, *107*, 3032. (b) Cossi, M.; Barone, V.; Mennucci, B.; Tomasi, J. *Chem. Phys. Lett.* **1998**, *286*, 253. (c) Mennucci, B.; Tomasi, J. *J. Chem. Phys.* **1997**, *106*, 5151.

(32) Tomasi, J.; Mennucci, B.; Cammi, R. *Chem. Rev.* **2005**, *105*, 2999.

(33) Cossi, M.; Scalmani, G.; Rega, N.; Barone, V. *J. Chem. Phys.* **2002**, *117*, 43.

(23) Gaussian 03, Revision C.02: Frisch, M. J.; Trucks, G. W.; Schlegel, H. B.; Scuseria, G. E.; Robb, M. A.; Cheeseman, J. R.; Montgomery, J. A., Jr.; Vreven, T.; Kudin, K. N.; Burant, J. C.; Millam, J. M.; Iyengar, S. S.; Tomasi, J.; Barone, V.; Mennucci, B.; Cossi, M.; Scalmani, G.; Rega, N.; Petersson, G. A.; Nakatsuji, H.; Hada, M.; Ehara, M.; Toyota, K.; Fukuda, R.; Hasegawa, J.; Ishida, M.; Nakajima, T.; Honda, Y.; Kitao, O.; Nakai, H.; Klene, M.; Li, X.; Knox, J. E.; Hratchian, H. P.; Cross, J. B.; Adamo, C.; Jaramillo, J.; Gomperts, R.; Stratmann, R. E.; Yazyev, O.; Austin, A. J.; Cammi, R.; Pomelli, C.; Ochterski, J. W.; Ayala, P. Y.; Morokuma, K.; Voth, G. A.; Salvador, P.; Dannenberg, J. J.; Zakrzewski, V. G.; Dapprich, S.; Daniels, A. D.; Strain, M. C.; Farkas, O.; Malick, D. K.; Rabuck, A. D.; Raghavachari, K.; Foresman, J. B.; Ortiz, J. V.; Cui, Q.; Baboul, A. G.; Clifford, S.; Cioslowski, J.; Stefanov, B. B.; Liu, G.; Liashenko, A.; Piskorz, P.; Komaromi, I.; Martin, R. L.; Fox, D. J.; Keith, T.; Al-Laham, M. A.; Peng, C. Y.; Nanayakkara, A.; Challacombe, M.; Gill, P. M. W.; Johnson, B.; Chen, W.; Wong, M. W.; Gonzalez, C.; Pople, J. A. Gaussian, Inc., Wallingford, CT, 2004.

(24) Hehre, W. J.; Radom, L.; Schleyer, P. v. R.; Pople, J. A. *Ab Initio Molecular Orbital Theory*; John Wiley & Sons: New York, 1986.